Supplement of

Two distinct modes of North American spring temperature evolution shaped by tropical SST regimes and midlatitude circulation

Wogu Zhong[1,2], Mingfang Ting[2], and Zhiwei Wu[1,3]

[1] Department of Atmospheric and Oceanic Sciences & Institute of Atmospheric Sciences / Key Laboratory of Polar Atmosphere-ocean-ice System for Weather and Climate, Ministry of Education / Shanghai Key Laboratory of Ocean-land-atmosphere Boundary Dynamics and Climate Change, Fudan University, Shanghai, 200438, China

[2] Lamont-Doherty Earth Observatory, Columbia University, Palisades, New York, 10964, United States of America

[3] IRDR ICoE on Risk Interconnectivity and Governance on Weather/Climate Extremes Impact and Public Health, Fudan University, Shanghai, 200438, China

Correspondence to: Wogu Zhong (wz2758@columbia.edu; wgzhong19@fudan.edu.cn); Mingfang Ting (ting@ldeo.columbia.edu)

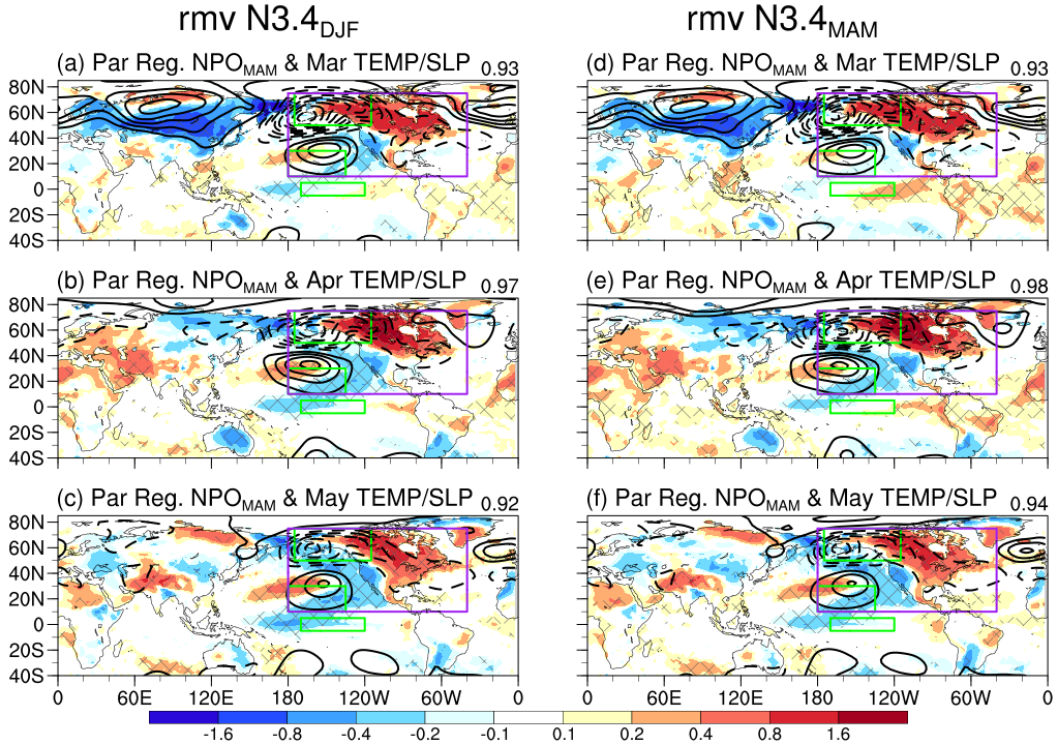

Figure S1: (a–c) Temperature anomalies (shading; unit: °C per standard deviation of the regressed index; with SST over ocean and SAT over land), SLP anomalies (black contours; unit: hPa per standard deviation of the regressed index; 0.5 hPa interval with zero contour omitted), and 925-hPa wind anomalies (vectors; unit: m/s per standard deviation of the regressed index; vectors plotted only in the tropics) in **(a)** March, **(b)** April, and **(c)** May regressed onto the standardized spring NPO index after removing the linear influence of the standardized winter Niño3.4 index (see *Methods*). All fields are linearly detrended prior to partial regression. Cross-hatching indicates regions where the regressed temperature anomalies are significant at the 95% confidence level based on a two-tailed Student's *t* test. Green boxes over the North Pacific denote the regions used to define the NPO, while the one over the tropical Pacific denotes the Niño3.4 region. The purple box outlines North America. Numbers in the top-right corner of each panel indicate the pattern correlation coefficients between North American SAT anomalies regressed onto the standardized spring NPO index after removing the linear influence of the standardized winter Niño3.4 index and those regressed onto the standardized PC1. **(d–f)** Same as **(a–c),** but for anomalies regressed onto the standardized spring NPO index after removing the linear influence of the standardized spring Niño3.4 index. Numbers in the top-right corner of each panel indicate the pattern correlation coefficients between North American SAT anomalies regressed onto the standardized spring NPO index after removing the linear influence of the standardized spring Niño3.4 index and those regressed onto the standardized PC1.

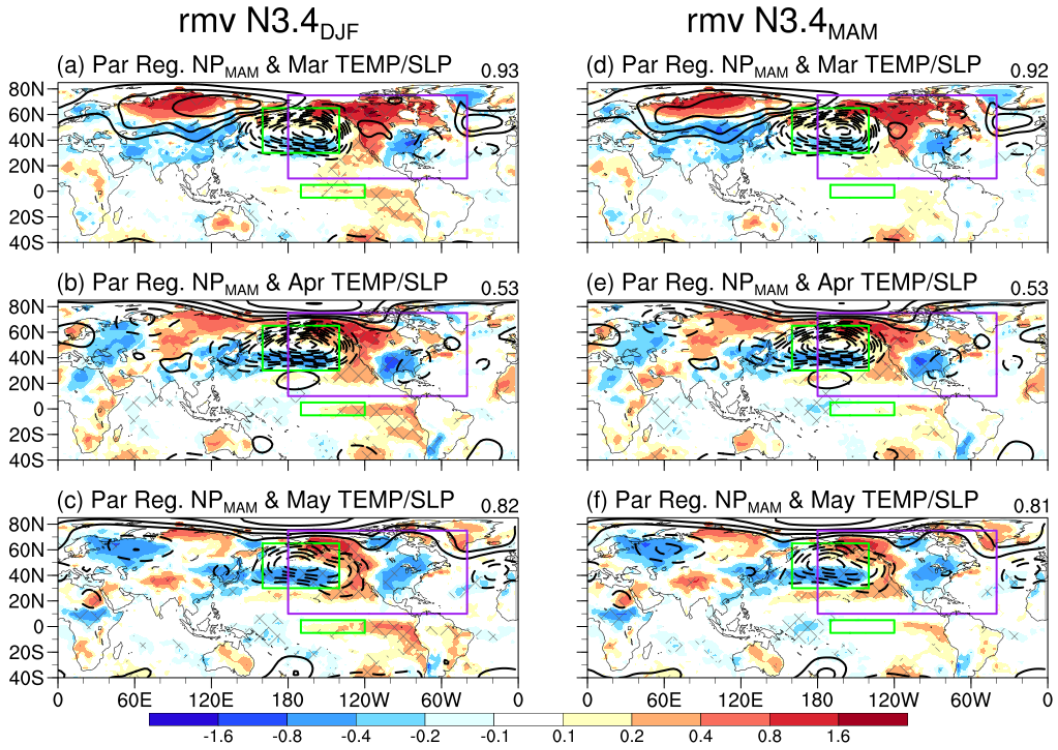

Figure S2: (a–c) Temperature anomalies (shading; unit: °C per standard deviation of the regressed index; with SST over ocean and SAT over land), SLP anomalies (black contours; unit: hPa per standard deviation of the regressed index; 0.5 hPa interval with zero contour omitted), and 925-hPa wind anomalies (vectors; unit: m/s per standard deviation of the regressed index; vectors plotted only in the tropics) in **(a)** March, **(b)** April, and **(c)** May regressed onto the standardized spring NP index after removing the linear influence of the standardized winter Niño3.4 index (see *Methods*). All fields are linearly detrended prior to partial regression. Cross-hatching indicates regions where the regressed temperature anomalies are significant at the 95% confidence level based on a two-tailed Student's *t* test. The green box over the North Pacific denotes the regions used to define the NP, while the one over the tropical Pacific denotes the Niño3.4 region. The purple box outlines North America. Numbers in the top-right corner of each panel indicate the pattern correlation coefficients between North American SAT anomalies regressed onto the standardized spring NP index after removing the linear influence of the standardized winter Niño3.4 index and those regressed onto the standardized PC2. **(d–f)** Same as **(a–c),** but for anomalies regressed onto the standardized spring NP index after removing the linear influence of the standardized spring Niño3.4 index. Numbers in the top-right corner of each panel indicate the pattern correlation coefficients between North American SAT anomalies regressed onto the standardized spring NP index after removing the linear influence of the standardized spring Niño3.4 index and those regressed onto the standardized PC2.

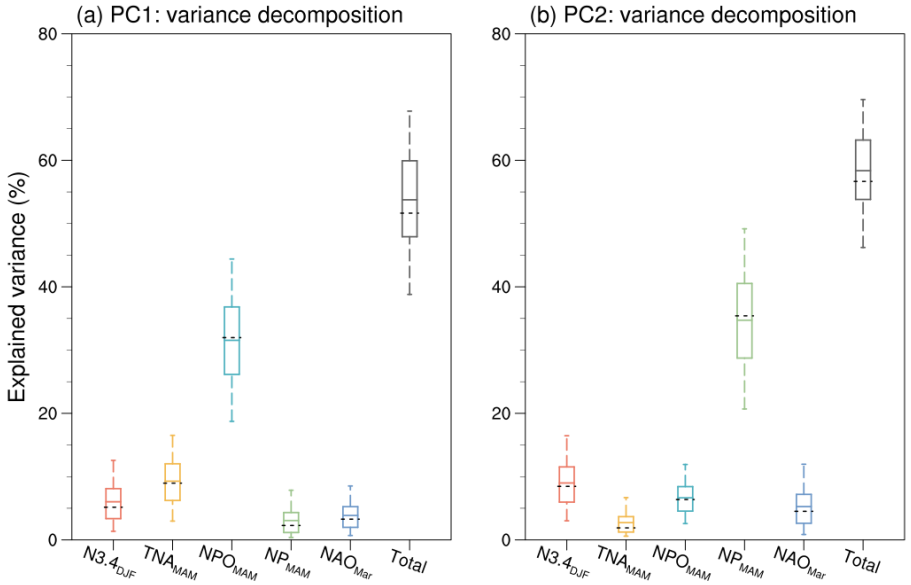

Figure S3: (a–b) Variance decomposition (dominance analysis) of the winter Niño3.4 index, the spring TNA index, the spring NPO index, the spring NP index, and the early spring NAO index (first five columns), along with their total contribution (sixth column), in explaining **(a)** PC1 and **(b)** PC2, based on a bootstrap method with 10,000 resamples. Boxplots represent the distribution of each variable's contribution across bootstrap resamples: the box spans the interquartile range (25th–75th percentiles), the solid line within the box denotes the median, and the whiskers indicate the 5th and 95th percentiles. The horizontal black dashed line indicates the contribution estimated from the original (non-bootstrap) samples.

Methods

Partial regression analysis

To isolate the impacts of midlatitude circulation patterns on SAT anomalies independent of ENSO, we perform a partial regression analysis as follows:

$$SAT_m = \alpha_m Niño_{3.4} + \varepsilon_m$$

where SAT_m denotes SAT anomalies at a given grid point, α_m is the regression coefficient, and ε_m is the residual representing the non-ENSO component of SAT anomalies. The intercept is omitted for simplicity.

The residual ε_m is further regressed onto midlatitude circulation indices:

$$\varepsilon_m = \beta_m NPO + \delta_m$$

$$\varepsilon_m = \gamma_m NP + \delta'_m$$